A Unidirectional Single-Phase LLC Based High Frequency Link Inverter

Anirban Pal, Vishal Anand AG, Bala Subrahmanyam Kuchibhatla and Kaushik Basu
Department of Electrical Engineering,
Indian Institute of Science, Bangalore
Bangalore-560012, India
{anirbanp, kbasu}@iisc.ac.in

***Abstract*—This paper presents a resonant LLC based isolated single-phase DC-AC converter for grid connected photovoltaic systems. The converter employs a LLC DC-rectified AC stage followed by a line frequency unfolder. A constant switching frequency based modulation strategy is used to generate sinusoidal output voltage. The gain of the converter is independent of the load current in the operating region. To control active power flow, a small variation in gain is needed which results in small variation in operating frequency. This ensures optimal design of the magnetic components. A closed form expression of the converter voltage gain is derived. Additionally, load independent ZVS of the input H-bridge is ensured. A 2 kW prototype is designed and key simulation and experimental results are presented to verify the converter operation.**

***Index Terms*—Resonant converter, LLC, unfolder circuit, isolated DC-AC converter, zero voltage switching, voltage gain.**

I. Introduction

The unidirectional high-frequency-link DC-AC converters are becoming popular for applications like grid integration of photovoltaic systems and fuel cells [1], [2]. The high frequency galvanic isolation provides high power density, light weight converter solution. The transformer is used for voltage matching, to reduce leakage current and to ensure safety. Generally these converters employ multi-stage power conversion system where a pulse width modulated (PWM) isolated DC-DC converter is followed by a DC-AC stage, connected through inter-stage DC link filter capacitor [3]. Recently a number of single stage solutions are reported which remove interstage filter capacitor [4], [5]. The PWM based topologies are widely popular due to fixed frequency operation and simple, essentially load independent control of the voltage gain. But the converters are either hard switched or have load dependent limited soft-switching range [5]. Additionally, the semiconductor devices experience high voltage stress due to circuit parasitics and the converters have high EMI emission [6].

The resonant based isolated DC-AC converters are widely investigated in literature [6]. The use of resonant tank can ensure wide, load-independent soft-switching range and reduces EMI emission. But wide variation of the switching frequency is required to generate the sinusoidal output voltage [2]. This results in non optimal magnetics design and complex control. Additionally, the voltage gain of these converters is load dependent and require variable frequency operation for output regulation. [7], [8] reported series and parallel resonant based DC-AC converter solutions. Here fixed frequency based modulation techniques are presented to generate sinusoidal output voltage. However wide variation of the switching frequency is still required as the voltage gain is load dependent. Additionally, these converters require a split input DC bus with two input DC link capacitors and employ a pair of resonant tank elements. [6] presents a LLC based inverter with unfolder circuit. But the converter operation is not discussed in details.

In this paper a LLC resonant based isolated DC-AC converter is proposed (Fig. 1a). The proposed topology with suggested modulation scheme has following features. (a) The converter employs a LLC DC-rectified AC stage followed by a line frequency unfolder. (b) The converter does not require a split DC bus and employs lower number of resonant tank elements [7], [8]. (c) The two legs of the input H-bridge are switched at slightly different but constant frequencies (close to resonant frequency) to generate sinusoidal output voltage. (d) The input bridge is zero voltage switched (ZVS). (e) In the operating region, the voltage gain and ZVS is load-independent. (f) To compensate the line impedance drop, a small variation in voltage gain is needed resulting in small variation in the operating frequency range. (g) This ensures optimal design of the magnetic elements. (h) A closed form expression of the converter voltage gain is derived. A 2 kW prototype is designed and key simulation results are presented to verify the operation.

II. Steady State Operation and Analysis

A. Modulation strategy

Fig. 1a shows the LLC based isolated DC-AC converter. In the DC side, the converter has a H-bridge ($S_1 - S_4$) followed by resonant tank elements L_r and C_r. A high frequency transformer with turns ratio $1 : n_r$ and magnetising inductance L_m is employed followed by a diode bridge rectifier ($D_1 - D_4$) and an unfolder ($Q_1 - Q_4$). The output of the unfolder is connected to a filter capacitor (C_f) before connecting it to the grid (v_g) through a line inductor (L_g). The resonating frequency of the tank, $f_r = \frac{1}{\sqrt{L_r C_r}}$. The half bridge legs are complementary switched with the gating pulses of 50% duty ratio. $S_1 - S_2$ and $S_3 - S_4$ are switched at frequencies $f_1 = (f_c + f_o)$ and $f_2 = (f_c - f_o)$ respectively (see Fig. 1c). The carrier frequency f_c is close to f_r, whereas f_o is the

2022 IEEE Energy Conversion Congress and Exposition (ECCE) | 978-1-7281-9387-8/22/$31.00 ©2022 IEEE | DOI: 10.1109/ECCE50734.2022.9947811

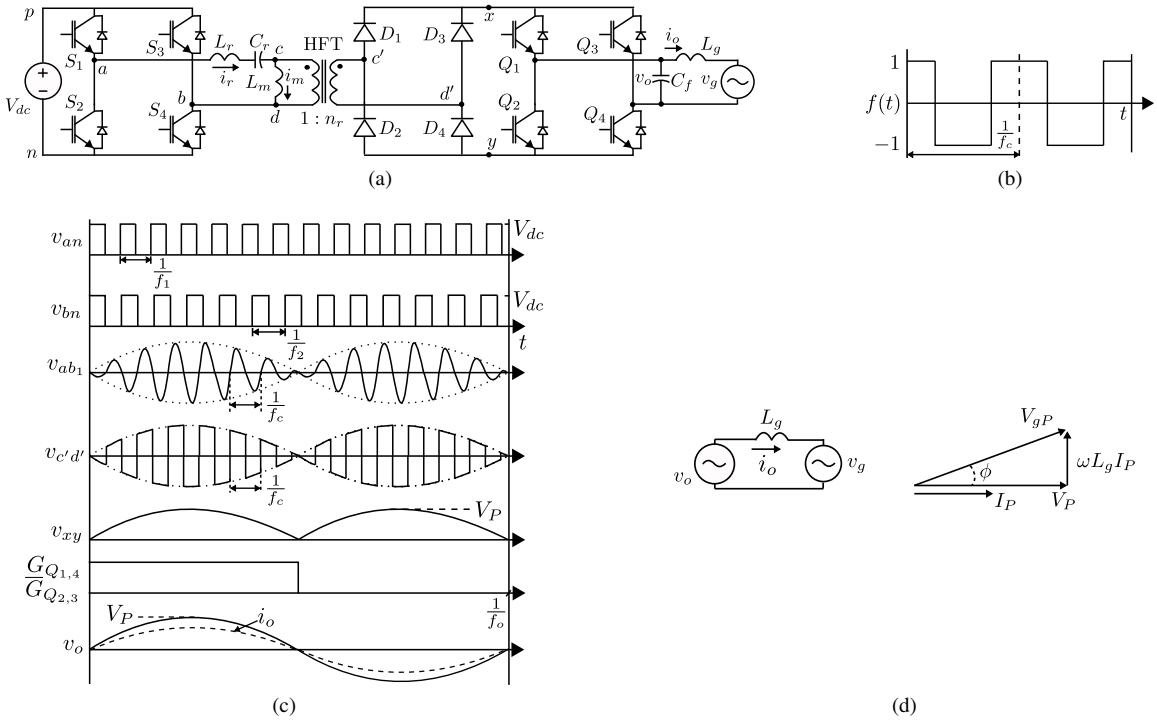

Fig. 1. (a) LLC based DC-AC converter, (b) key waveforms, (c) function $f(t)$, (d) equivalent circuit of the grid connected converter and phasor diagram

fundamental frequency of grid voltage v_g. The primary bridge pole voltages are given as in (1).

$$\begin{aligned} v_{an} &= \frac{V_{dc}}{2} + \sum_{n=1,3,5..} \frac{2V_{dc}}{n\pi} \sin n(\omega_c + \omega_o)t \\ v_{bn} &= \frac{V_{dc}}{2} + \sum_{n=1,3,5..} \frac{2V_{dc}}{n\pi} \sin n(\omega_c - \omega_o)t \end{aligned} \tag{1}$$

The tank input voltage v_{ab} is given in (2). Here $\omega(=2\pi f)$ is the angular frequency.

$$v_{ab} = (v_{an} - v_{bn}) = \sum_{n=1,3,5..} \frac{4V_{dc}}{n\pi} \cos n\omega_c t \sin n\omega_o t \tag{2}$$

The fundamental component of the tank input is $v_{ab_1} = \frac{4V_{dc}}{\pi} \cos\omega_c t \sin\omega_o t$ (shown in Fig. 1c). As, $\omega_c \approx \omega_r$, the resonant tank filters out the other high frequency components and only allows the fundamental component (v_{ab_1}) to pass. In the secondary, the high frequency AC is rectified by the diode bridge ($D_1 - D_4$) and then it is line frequency inverted by the unfolder $Q_1 - Q_4$. C_f filters out the high frequency ripple current. The desired output voltage is given in (3) (see Fig. 1c).

$$v_o = V_P \sin\omega_o t \tag{3}$$

V_P is the peak value of the output voltage.

The transformer secondary voltage, $v_{c'd'}$ is shown in Fig. 1c. When $\omega_c \approx \omega_r$, $v_{c'd'} \approx v_o \cdot f(t)$.

$$f(t) = \sum_{n=1,3,5..} \frac{4}{n\pi} (-1)^{\frac{n-1}{2}} \cos n\omega_c t \tag{4}$$

$f(t)$ is given in (4) (see Fig. 1b). Hence $v_{c'd'}$ can be approximately expressed as in (5).

$$v_{c'd'} \approx \sum_{n=1,3,5..} \frac{4V_p}{n\pi} (-1)^{\frac{n-1}{2}} \cos n\omega_c t \sin\omega_o t \tag{5}$$

The fundamental component of the transformer primary voltage $v_{cd_1} = \frac{4V_p}{n_r\pi} \cos\omega_c t \sin\omega_o t$, has similar expression as v_{ab_1}. To control V_P, f_c will be varied below f_r. But the assumption, $f_c \approx f_r$ will still be valid. Next, the relationship between V_P and f_c is analysed.

B. Relation between V_P and f_c

From (2), v_{ab} at $\omega_o t = \frac{\pi}{2}$ is given as in (6).

$$v_{ab} = \sum_{n=1,3,5..} \frac{4V_{dc}}{n\pi} (-1)^{\frac{n-1}{2}} \cos n\omega_c t = V_{dc} \cdot f(t) \tag{6}$$

As $f_c \gg f_o$, near the peak of the output voltage (v_o), a square wave AC voltage with magnitude $\pm V_{dc}$ is applied at the tank input (v_{ab}). The the equivalent circuit is shown in Fig. 2a. Due to diode bridge, the converter supports only UPF operation. Hence, $i_o = I_P$ (which is peak value of load current) when $\omega_o t = \frac{\pi}{2}$. The operation of the converter is analysed at this instant.

For simplicity, the analysis is presented in per unit (PU) form. The key quantities are given in Table I. The PU quantities used in the analysis are- tank input voltage $m_{ab} = \frac{n_r v_{ab}}{V_b}$, resonant capacitor voltage $m_c = \frac{n_r v_{C_r}}{V_b}$, resonant inductor current $j_r = \frac{i_r}{n_r I_b}$, transformer magnetising current $j_m = \frac{i_m}{n_r I_b}$ and peak load current $J = \frac{I_P}{I_b}$. The gain-frequency (M-F) plot

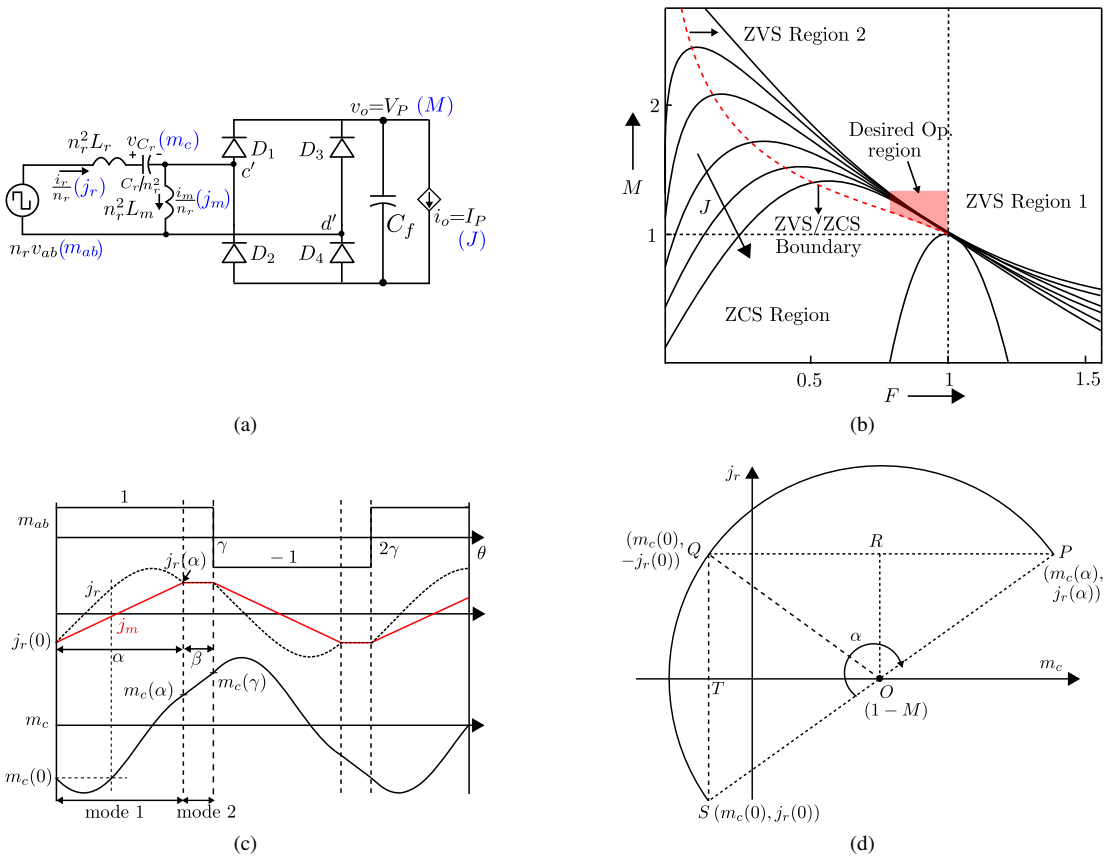

Fig. 2. (a) Equivalent circuit of the converter when $\omega_o t = \frac{\pi}{2}$ (b) Gain-Frequency plot of LLC converter, (c) LLC waveforms when $F < 1$, (d) State plane diagram in mode 1

TABLE I
KEY QUANTITIES OF THE LLC CONVERTER

Parameter	Values
Base voltage, V_b	$n_r V_{dc}$
Base impedance, R_b	$n_r^2\sqrt{\frac{L_r}{C_r}}$
Base current, I_b	$\frac{V_b}{R_b}$
Inductance ratio , σ	$\frac{L_m}{L_r}$
Frequency ratio, F	$\frac{f_c}{f_r}$
Voltage gain, M	$\frac{V_P}{V_b}$
Angular half period, γ	$\frac{\pi}{F}$

of a LLC converter is shown in Fig. 2b [9]. To achieve zero voltage switching (ZVS) of the primary bridge and higher gain, the converter is operated with $F < 1$. Fig. 2b shows the desired operating region in red shade (considering required variation of M is small. The reason is explained in next section). Here, the required variation of f_c will be small and F will be close to unity. When $F < 1$, the LLC operates in DCM mode. Here the objective is to find out a closed form expression of M as a function of F using state-plane analysis. Fig. 2c shows key waveforms of the converter. The converter operation is symmetrical over one half of the carrier cycle. The converter has two modes of operations- mode 1 ($0 \leq \theta \leq \alpha$) and mode 2 ($\alpha \leq \theta \leq \gamma$) where $\theta = \omega_r t$.

1) Mode-1: In mode 1, the diode bridge conducts the output current. The circuit equations are given as in (7).

$$\begin{aligned} \frac{dj_r}{d\theta} + m_c &= 1 - M \\ \frac{dm_c}{d\theta} &= j_r \\ \sigma\frac{dj_m}{d\theta} &= M \end{aligned} \tag{7}$$

So using (7), in this mode, $j_m(\alpha) - j_m(0) = \frac{M\alpha}{\sigma}$. Due to symmetry in the waveform (see Fig. 2c), $j_m(\alpha) = -j_m(0)$ and thus $j_m(\alpha) = \frac{M\alpha}{2\sigma}$. At the end of this mode the diode bridge stops conducting. Hence $j_r(\alpha) = j_m(\alpha)$.

2) Mode-2: In mode 2 the circuit operates in DCM and the load current is supplied by the output capacitor C_f. The presented analysis considers L_m to be large and hence the variation of j_m is negligible. So $j_r(\gamma) = j_m(\gamma) = j_m(\alpha)$. In this mode, m_c varies linearly as $\frac{dm_c}{d\theta} = j_m(\alpha)$. At steady state operation due to the symmetry in the waveforms, $m_c(\gamma) = -m_c(0)$ and $j_r(\gamma) = -j_r(0) = -j_m(0)$.

III. CONVERTER DESIGN AND SIMULATION RESULTS

Fig. 2d shows the state plane diagram of the resonant tank variables, j_r and m_c in mode 1. Using basic trigonometric concepts, from Fig. 2d it can be shown that, $\triangle ORQ \equiv \triangle ORP$

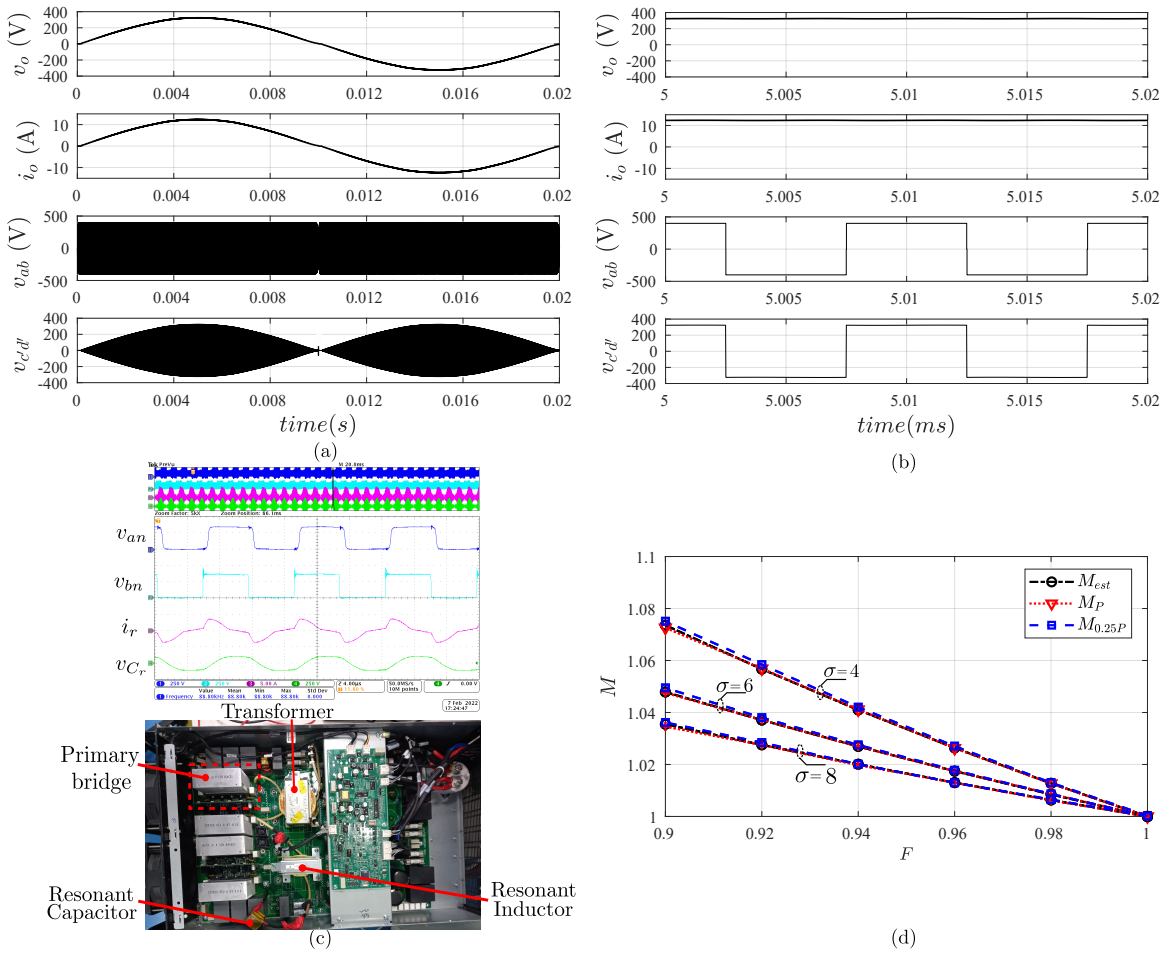

Fig. 3. Simulation results-(a) line cycle waveforms (v_o, i_o), (b) switching cycle waveforms at $\omega_o t = \frac{\pi}{2}$, (c) experimental setup and experimentally obtained tank voltage and current waveforms and (d) M vs. F plot

and $\triangle OTQ \equiv \triangle OTS$. From the equal triangles, α can be estimated as $\alpha = \pi$. As $\triangle ORQ \equiv \triangle ORP \Rightarrow RP = RQ \Rightarrow m_c(\alpha) + m_c(0) = 2 - 2M$. In mode 2, $m_c(\gamma) - m_c(\alpha) = j_m(\alpha)(\gamma - \alpha) \Rightarrow m_c(\alpha) + m_c(0) = -\frac{M\alpha}{2\sigma}(\gamma - \alpha)$. By equating above two equations, the converter gain M can be expressed as in (8). .

$$M = \frac{4\sigma F}{4\sigma F - \pi^2(1-F)} \tag{8}$$

Thus the peak value (V_P) of the out voltage (v_o) is given as in (9).

$$V_P = n_r M V_{dc} = \frac{4 n_r \sigma F V_{dc}}{4\sigma F - \pi^2(1-F)} \tag{9}$$

A. Power flow control

Due to the secondary diode bridge, the converter supports only instantaneous unidirectional power flow from DC to AC. Hence the output voltage v_o and line current i_o must be in same phase. Fig. 1d shows the equivalent circuit of the converter connected to the grid and the phasor diagram for the fundamental (f_o) components. V_P, V_{gP} and I_P are peak values of v_o, v_g and i_o respectively. ϕ is the phase angle. For a given power flow P, V_P and ϕ can be obtained by solving (10).

$$\begin{aligned} P &= 0.5 V_P I_P = 0.5 V_{gP} I_P \cos\phi \\ V_P^2 &+ (\omega_o L_g I_P)^2 = V_g^2 \end{aligned} \tag{10}$$

V_P and ϕ can be expressed as given in (11).

$$\begin{aligned} V_P &= \sqrt{0.5\left(V_{gP}^2 + \sqrt{V_{gP}^4 - (2\omega_o L_g P)^2}\right)} \\ \phi &= \cos^{-1}\frac{V_P}{V_{gP}} \end{aligned} \tag{11}$$

The power flow, P can be controlled by changing V_P and ϕ. If we considered $V_{gP} = 1$ PU, rated power $P = 1$ PU and 10% line impedance (PU $\omega_o L_g = 0.1$), the estimated $V_P = 0.995$ and $\phi = 5.77°$. When $P = 0.2$ PU, estimated $V_P = 0.9998$ and $\phi = 1.15°$. The change in V_P with the variation of P is very small. Hence the converter can be designed to operate close to resonant frequency i.e. $f_c \simeq f_r$. Additionally if we consider a 10% variation in v_g, let $V_{gP} = 1.1$PU$\Rightarrow V_P = 1.096$ PU at rated power. For a design with $\sigma = 4$, using (8) $F = 0.875$ i.e. f_c is still close to f_r.

TABLE II
CONVERTER SPECIFICATION

Parameter	Values
DC input (V_{dc})	400V
Grid voltage peak (V_{gP})	$230\sqrt{2}$V
Grid frequency (f_o)	50Hz
Output power (P)	2kW
Resonant frequency f_r	100kHz
Filter capacitance C_f	5μF

B. Design Steps

The specification of the converter is given in Table II. The following design steps determine the values of L_r, C_r and n_r in Fig. 1a. At rated power (using expression of V_P given in (11)) estimated $V_P = 0.995 \times 230\sqrt{2}$=228.835$\sqrt{2}$ and $I_P = \frac{2P}{V_P} = 12.36$A. At rated power, we have considered $J = 1$, $f_c = f_r$ =100kHz i.e. $F = 1$. The primary leg $S_1 - S_2$ is switched at $(f_c + f_o) = 100050$Hz where as $S_3 - S_4$ is switched at $(f_c - f_o) = 99950$Hz. Using (8), for $F = 1$, M can be estimated as $M = 1$. Hence the transformer turns ratio $n_r = \frac{V_P}{MV_{dc}} = 0.809$. As $J = \frac{I_p R_b}{n_r V_{dc}} = 1$, $R_b = n_r^2\sqrt{\frac{L_r}{C_r}} = 26.18\Omega$. The resonant frequency $f_r = \frac{1}{2\pi\sqrt{L_r C_r}} = 100$kHz. Thus $L_r = 63.3\mu$H and $C_r = 40n$F. To limit the circulation current, σ is chosen as $\sigma \geq 4$. If we consider $\sigma = 4$, $L_m = \sigma \cdot L_r = 253.2\mu$H.

C. Simulation and experimental results

The converter is simulated for the operating condition given in Table II. Fig. 3a shows the 50Hz sinusoidal output voltage and current waveforms with peak values 323.6V and 12.35A respectively. Tank input voltage (v_{ab}) and Transformer secondary voltage ($v_{c'd'}$) are also shown in this figure. Simulated waveforms are matched with Fig. 1c. Same set of waveforms are presented in Fig. 3b over two switching cycles (100kHz) when $\omega_o t = \frac{\pi}{2}$. v_{ab} and $v_{c'd'}$ are square waves with magnitude $\pm$400V and $\pm$323.6V respectively. Fig. 3c shows experimental setup and experimentally obtained tank circuit waveforms. As $L_m = 4L_r$, i_m is significantly smaller than i_r. Peak value of the resonant capacitor voltage (v_{C_r}) is 650V. Fig. 3d shows $M - F$ plots for $\sigma = 4, 6, 8$ and $0.9 \leq F \leq 1$. M_{est} is the estimated values of M using (8). M_P and $M_{0.5P}$ are the values of M, obtained from simulation at rated power and 25% of the rated power respectively. Fig. 3d validates (8) and also shows that peak output voltage (V_P) is almost independent of load current in the considered region.

IV. CONCLUSION

This paper presents a LLC based unidirectional, isolated DC-AC converter topology for grid connected PV systems and fuel cells. The proposed modulation strategy ensures fixed frequency operation of the LLC input bridge to generate the sinusoidal output voltage. In the operating region, the converter voltage gain is load-independent. But to compensate the line impedance drop, a small variation in voltage gain is needed resulting in small variation in the operating frequency range. The operation ensures load independent ZVS of the input H-bridge. The grid interfaced H-bridge is line frequency switched incurring negligible switching loss. A brief discussion on converter operation along with key simulation results are given here.

REFERENCES

[1] B. K. Bose, P. M. Szczesny, and R. L. Steigerwald, "Microcomputer control of a residential photovoltaic power conditioning system," *IEEE Transactions on Industry applications*, no. 5, pp. 1182–1191, 1985.

[2] V. Anand, A. Pal, B. Kuchibhatla, R. Gurunathan, and K. Basu, "An unidirectional single stage single phase soft-switched resonant high frequency link inverter," *IEEE Transactions on Industry Applications*, 2021.

[3] S. Inoue and H. Akagi, "A bidirectional dc–dc converter for an energy storage system with galvanic isolation," *IEEE transactions on power electronics*, vol. 22, no. 6, pp. 2299–2306, 2007.

[4] A. Pal and K. Basu, "A partially soft-switched dc/ac high frequency link unidirectional converter for medium voltage grid integration," in *2015 National Power electronics Conference (NPEC)*, 2015.

[5] ——, "A unidirectional single-stage three-phase soft-switched isolated dc–ac converter," *IEEE Transactions on Power Electronics*, vol. 34, no. 2, pp. 1142–1158, 2018.

[6] X. Li and A. K. Bhat, "A comparison study of high-frequency isolated dc/ac converter employing an unfolding lci for grid-connected alternative energy applications," *IEEE transactions on power electronics*, vol. 29, no. 8, pp. 3930–3941, 2014.

[7] V. Ranganathan, P. D. Ziogas, and V. R. Stefanovic, "A dc-ac power conversion technique using twin resonant high-frequency links," *IEEE Transactions on Industry Applications*, no. 3, pp. 393–400, 1983.

[8] G. C. Knabben, D. Neumayr, and J. W. Kolar, "Constant duty cycle sinusoidal output inverter with sine amplitude modulated high frequency link," in *2018 IEEE Applied Power Electronics Conference and Exposition (APEC)*. IEEE, 2018, pp. 2521–2529.

[9] X. Fang, H. Hu, Z. J. Shen, and I. Batarseh, "Operation mode analysis and peak gain approximation of the llc resonant converter," *IEEE transactions on power electronics*, vol. 27, no. 4, pp. 1985–1995, 2011.